ACS Medicinal Chemistry Letters

Letter

Cite This: ACS Med. Chem. Lett. 2018, 9, 193−197

Water Solubility Enhancement of Pyrazolo[3,4-*d*]pyrimidine Derivatives via Miniaturized Polymer−Drug Microarrays

Monica Sanna,[†] Giovanna Sicilia,[‡] Ali Alazzo,[‡] Nishant Singh,[‡] Francesca Musumeci,[†] Silvia Schenone,[†] Keith A. Spriggs,[‡] Jonathan C. Burley,[‡] Martin C. Garnett,[‡] Vincenzo Taresco,*[,‡] and Cameron Alexander*[,‡]

[†]Dipartimento di Farmacia, Università degli Studi di Genova, Viale Benedetto XV 3, 16132 Genova, Italy

[‡]School of Pharmacy, University of Nottingham, University Park, Nottingham NG7 2RD, U.K.

Supporting Information

ABSTRACT: A miniaturized assay was optimized to evaluate the enhanced apparent water solubility of pyrazolo[3,4-*d*]pyrimidine derivatives used extensively as anticancer drug scaffolds. The applied amount of drugs used in the reported strategy ranged from 5 to 10 μg per formulation which were dispensed by an inkjet 2D printer directly into a 96-well plate. The selected polymer/drug formulations with high water solubility demonstrated improved cytotoxicity against a human lung adenocarcinoma cancer cell line (A549) compared to the free drugs. We attribute the enhanced efficacy to the improved apparent-solubility of the drug molecules achieved via this methodology. This novel miniaturized method showed promising results in terms of water solubility improvement of the highly hydrophobic pyrazolo[3,4-*d*]pyrimidine derivatives, requiring only a few micrograms of each drug per tested polymeric formulation. In addition, the reported experimental evidence may facilitate identification of suitable polymers for combination with drug, leading to investigations on biological properties or mechanisms of action in a single formulation.

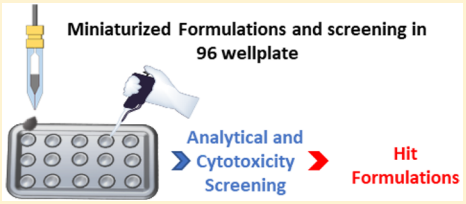

KEYWORDS: *Miniaturized assay, inkjet 2D printing, amorphous solid dispersion, water solubility enhancement and pyrazolo[3,4-d]pyrimidines*

The pyrazolo[3,4-*d*]pyrimidine (p[3,4]p) nucleus (Figure 1(a)) is an adenine isostere, and it can therefore mimic adenine in the catalytic sites of many oncogenic kinases which act on ATP. For these reason p[3,4]p has received growing attention as a scaffold for the combinatorial synthesis of drug candidates, particularly in targeted anticancer therapy based on protein kinase inhibitors.[1−5] Many p[3,4]p derivatives act as nanomolar inhibitors both of the cytoplasmic tyrosine kinases SRC, ABL1, and FYN[6,7] and of the serine-threonine kinase SGK1.[8] In addition, this family of compounds also showed an enhanced antiproliferative profile against several cancer cell lines, including those derived from neuroblastoma,[9] chronic myeloid leukemia,[10] glioblastoma,[11] rhabdomyosarcoma,[12] osteosarcoma,[13] prostate cancer[14] and mesothelioma.[15]

Although these molecules are readily soluble in DMSO and other organic solvents, limited solubility in water adversely affects their bioavailability and efficacy. Thus, in order to avoid the use of toxic organic solvents for *in vitro* and *in vivo* tests, several strategies have been sought to improve the aqueous solubility and pharmacokinetics of p[3,4]p derivatives, such as formation of complexes with cyclodextrins,[16] encapsulation into liposomes,[17] formulation with albumin into nanoparticles,[18] and synthesis of prodrug derivatives.[19]

However, one of the simplest and most promising methods is to create an amorphous solid dispersion where the drug is molecularly dispersed in an inert carrier, typically a hydrophilic polymer,[20−22] such that the resulting stabilized amorphous drug shows a higher water apparent-solubility compared to the crystal form.[23]

Accordingly, we have previously developed a novel miniaturized printing technology as a screening method to evaluate drug−polymer compatibility.[24] This new technique represents an efficient method to evaluate pharmaceutical formulations and assess the compatibility between drug and polymer. It requires only nanogram quantities of materials which results in about 6 orders of magnitude lower amount of active pharmaceutical ingredient (API) compared to conventional methods. In this regard, routinely analytical techniques such as DSC and XRPD need milligrams of samples to evaluate drug−polymer blend stability.

Here we report, for the first time, an efficient inkjet 2D printer-based screening process to identify the best polymeric carriers for aqueous solubilization of different p[3,4]p derivatives at minimal sample amounts. We demonstrate a complete miniaturized and fast analytical route to determine polymer−drug formulations for hit derivatives and validate this approach in a standard cytotoxicity screening.

Received: November 1, 2017
Accepted: January 29, 2018
Published: January 29, 2018

DOI: 10.1021/acsmedchemlett.7b00456
ACS Med. Chem. Lett. 2018, 9, 193−197

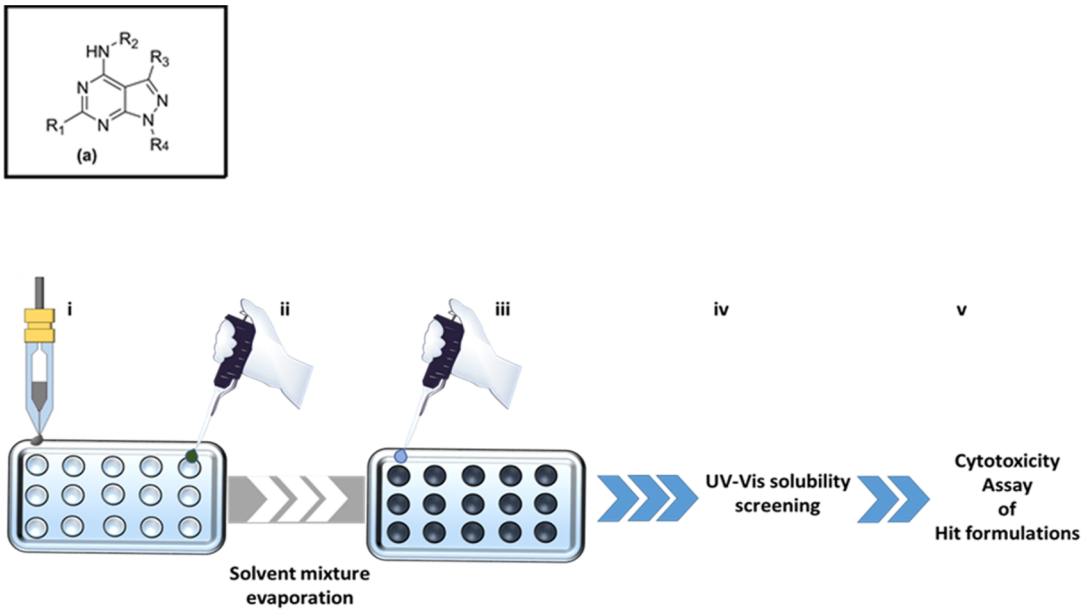

Figure 1. (a) General structure of pyrazolo[3,4-*d*] pyrimidines. (i) High-throughput dispensing of DMSO drug solutions by an inkjet 2D printer. (ii) Sequential addition of polymeric aqueous solutions and evaporation of water and DMSO. (iii) Resuspension with water of the dry solid dispersions. (iv) Evaluation of the apparent-solubility of the drugs in water from the polymeric matrixes via multiwell-reader UV−vis analysis. (v) MTT-cytotoxicity assessment of the hit formulations.

The initial work involved selection of five previously reported p[3,4]p, compounds **1**−**5**[7,15,16,25,26] (Figure 1SI) and synthesis of one new molecule, compound **6**. These candidate drugs were combined with seven different commercially available hydrophilic polymers selected from those commonly used as pharmaceutical excipients (Figure 1SI). The initial drug and polymer stock solutions were prepared by dissolving the drugs in DMSO and the polymers in deionized (DI) water, in order to reach final concentrations 10 and 1 mg/mL, respectively. Initially, a fixed volume of each drug solution was dispensed by a piezoelectric printer into a 96-well plate (each drug was formulated at a drug/polymer ratio of 10/90% w/w), used as printer target as well as a storage platform. DMSO droplets with nominal volumes ranging from 250 to 280 pL were dispensed to obtain a final amount of drug of 5−6 μg (Figure 1i). Subsequently (Figure 1ii), the different polymer solutions were pipetted into the different wells, by using a pipet (drug controls were prepared by simply adding water rather than polymer solutions). The well plates were left inside the printer cage to allow the DMSO−water mixture to slowly evaporate overnight at room temperature (from our previous experience,[24] the amount of DMSO dispensed, for each well in the present work, evaporates completely in the employed conditions). Subsequently, in order to remove any possible residual trapped solvent in the solid formulations, all the well plates were moved into a vacuum drying oven at room temperature for 2 days (Figure 1ii).

Generally, to dispense the complete set of 6 pure drugs and to pipet the 7 polymers in triplicate, the entire process required around 40 min and around 15−18 μg per drug. The drug−polymer solid formulations were then analyzed for solubility by resuspension in 200 μL of DI water (Figure 1iii). The quantitative determination of any UV−vis active molecule present in a solution (in this case the aromatic p[3,4]p derivatives) can be obtained by comparison with its calibration curve plotted using several solutions of known concentration. However, due to the low solubility and stability in water and DMSO, respectively, of the whole set of drugs, it was not possible to determine quantitatively the amount of soluble component. To overcome this problem in a pragmatic manner, an analytic screening based on the variation of the absorbance between the free drug redissolved in water and its polymer formulation was developed (Figure 1iv). This was achieved by normalizing the absorbance values of the drug−polymer dispersions against the absorbance of the free drug in water at the same maximum wavelength. The resulting values ($\Delta A\%$) were then used to compare the ability of the different polymers to solubilize the sample set of drugs. The absorbance ($A0$) of the drugs alone in water was evaluated by using a UV−vis multiwell plate reader, which was able to measure the full wavelength-spectrum in the range between 200 and 1000 nm in less than 30 s per sample. As anticipated, no signals were observed from the presence of water-insoluble drugs (Figure 2SI and 3SI). In parallel, the absorbance of the aqueous solutions of drug/polymer blends (A) was tested by using the absorbance of the polymer solutions as a blank (Figure 4SI). All the absorbance values were kept in the range $0 < A < 1$ where the Beer−Lambert law can be considered valid and, thus, the correlation between absorbance and drug concentration.

$$\Delta A\% = \frac{\Delta A}{A_0} \times 100 = \frac{(A - A_0)}{A_0} \times 100$$

Detailed data of $\Delta A\%$ values for each polymer−drug combination can be found in the Supporting Information (Table 1SI and Figures 5SI−6SI). It is apparent from these data that two surfactants (Pluronic F-68 and Tween 80) and the amphiphilic copolymer PVPVA showed notably higher $\Delta A\%$ average values compared to the homopolymers (PEG 8000−20000, PVP, and HPMC). Based on these data, $\Delta A\%$ average values were calculated and used to rank the polymers in terms of drug apparent-solubility enhancement (Figure 2). This was anticipated, since as a first assumption, the trend in solubilizing hydrophobic drugs might be attributed to the presence of

DOI: 10.1021/acsmedchemlett.7b00456
ACS Med. Chem. Lett. 2018, 9, 193−197

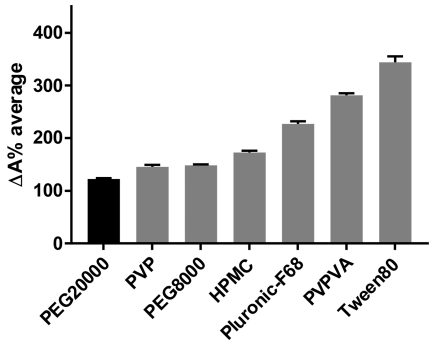

Figure 2. Δ*A*% average of polymers ranked according to their water apparent-solubility enhancement (high Δ*A*% is related with a high drug water solubility). Error bars showing standard deviation (n = 3).

hydrophobic blocks in Pluronic F-68, Tween 80, and PVPVA, which could participate in associative interactions with the drugs. However, it is also interesting to highlight that, in this first-generation array, PEG chain length also affected the overall drug apparent-solubility (Figure 2), which increased independently from the initial water solubility of the drugs (see Figure 3SI).

After this first analytical screening, on the basis of the Δ*A*% average results, each drug was formulated with two of the best performing polymers from the initial set, i.e. PVPVA, Pluronic F-68, and Tween 80 (Table 1SI).

The antiproliferative activity of the p[3,4]p derivatives alone or in combination with polymers was assessed against a human lung adenocarcinoma cell line (A549), due to its high cytosolic content of tyrosine and serine-threonine kinases (Figure 1v). As shown in Figure 3, none of the drugs formulated as aqueous

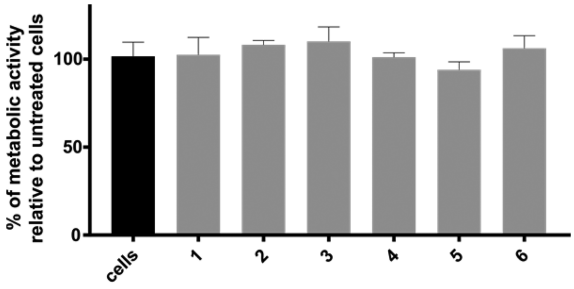

Figure 3. Cytotoxicity of pure drug solutions (30 μg/mL) against human lung adenocarcinoma cell line (A549). Due to the low solubility of the whole set of drugs, no antiproliferative activity was shown in the high-throughput MTT assay adopted. Error bars show standard deviation (n = 4).

suspensions was cytotoxic after 24 h treatment. Before screening the drug−polymer formulations, all the polymers were also tested at varying concentrations against the A549 cell line (Figure 7SI) to evaluate their cytotoxicity and identify the least toxic polymer concentration, in order to avoid any effects of the polymer carrier on the final formulation killing activity.

The data showed that the polymers were essentially nontoxic to A549 cells up to concentrations of 200 μg/mL. Subsequent solid dispersion cytotoxicity assays were therefore performed at polymer carrier concentrations below the threshold level of 200 μg/mL.

Printing of drugs into polymer dispersions at a level of 90% polymer and assays of these formulations with A549 cells showed growth inhibition of ∼20−50% (Figure 4), and more

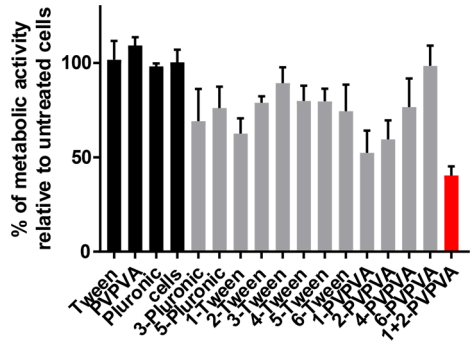

Figure 4. Cytotoxicity of selected prescreened formulations. The final drug concentration reached in the formulations was around 30 μg/mL, equal to a loading in the polymer matrix of 10% w/w. As shown in figure, polymers alone showed no adverse activity against the selected cell type. Red bar: cytotoxicity of **1** + **2**-PVPVA at 30 μg/mL in drugs (15 μg/mL, 15 μg/mL of **1** + **2**). Error bars show standard deviation (n = 4).

than the drugs alone at 30 μg/mL. These data also showed that compounds **1** and **2** were the most active drug candidates (Figure 4). We also used this formulation process to identify a pair of drugs to evaluate the combined effect of two more potent active principles in a single polymeric blend; thus, **1** (15 μg/mL) and **2** (15 μg/mL) were formulated with PVPVA (drug/polymer ratio constant at 10/90% w/w). As shown in Figure 4 (red bar) a synergistic effect of the combined formulation (**1** + **2**-PVPVA) was observed with respect to the single ones. In particular, a further 15−20% growth inhibition was reached (∼60% of killing effect). This experimental evidence may facilitate both the future adoption of drug combinations in the field of kinase inhibitors and dosage of drugs with different nature and/or mechanisms of action in one single formulation. To further validate this methodology, traditional cell viability assays using DMSO drug solutions were also performed (Figure 8SI). As can be seen in Figure 8SI, formulations gave similar or more accurate cytotoxicity results than that obtained with DMSO. These latter results not only support the analytical evidence of an improved drug water solubility after formulation but also support the enhancement of availability conferred by solid dispersions.

In an attempt to shed some light upon the interactions established between drug and polymer, some preliminary experiments were carried out using dynamic light scattering (DLS). This was carried out on just the most powerful single drug formulation (**1**-PVPVA) resulting from the biological screening reported in the present work (Figure 4). PVPVA showed a poor correlation curve indicating a highly disperse preparation, and the resulting DLS traces could be interpreted as a mixture of small and large polymer micelles. A similar poor correlation curve accompanied by the presence of big aggregates was observed for the free form of **1** as would be expected from its low solubility (Figure 9SI). On the other hand, the **1**-PVPVA formulation showed a single unimodal peak in the range of 1000 nm with a discrete dispersion (PDI of 0.4). As the only peak in this sample, this must be a mixture of both polymer and drug, hinting at a degree of interaction between the hydrophilic polymeric matrix and the hydrophobic drug (Figure 5 and Figure 9SI). The self-assembling of the **1**-PVPVA blend into nanomicro structures might explain not only the higher apparent-solubility of the formulation, compared to the free drug, but also the enhanced biological activity, due to a

DOI: 10.1021/acsmedchemlett.7b00456
ACS Med. Chem. Lett. 2018, 9, 193−197

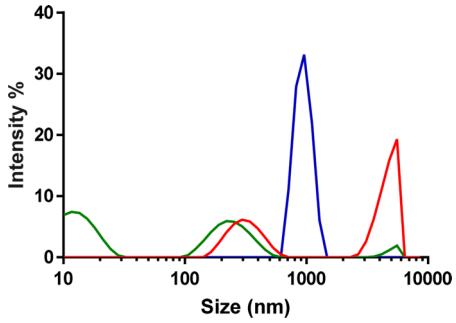

Figure 5. DLS traces in DI water of untreated **1** (red), PVPVA (green), and **1**-PVPVA (blue) as a formulation. Light scattering measurements were collected on suspensions prepared with a final concentration of 0.5 mg/mL in drug (concentration adopted due to instrumental detection limits).

higher bioavailability than the free drug. This result provides preliminary support for the effectiveness of the new method. However, a more rigorous study would be needed to prove the exact nature of polymer−drug interactions and the features of any structure in particles of the final blend.

It is worth remarking that the drugs alone have a really low water solubility (Figure 3SI), which reflects the neglectable availability in water (Figure 3), while, by formulating the p[3,4]p derivatives as reported in the present method, the molecules become more soluble and can support a concentration around 30 μg/mL for the cell assays.[26]

In conclusion, in the present work, we have developed a new miniaturized screening process, based on an inkjet printing technology, able to identify the best formulation to enhance the apparent water solubility of some p[3,4]p derivatives, active as kinase inhibitors. From the ΔA% as a single value for each combination drug−polymer or a ΔA% average value to rank the apparent-solubility enhancement, we have identified the best polymers able to solubilize the p[3,4]p in water. The low quantity of drugs used in the present experiments is one of the strongest points of the reported method. In fact, we have used in total less than 20 μg for each drug. This is crucial since the synthesis of these molecules encompasses difficult and time-consuming synthetic steps with long workup procedures and high organic solvent consumption. Moreover, with this strategy, it is possible to carry out biological tests for these drugs without direct drug dissolution in DMSO as required in previous work.[27] This method offers a powerful strategy to overcome the problem of the low solubility of this class of compounds and/or other systems involving different poorly water-soluble drugs. As a consequence, formulations can be readily identified for biological (*in vitro*−*in vivo*) studies and as a starting point for more detailed formulation work.

■ ASSOCIATED CONTENT

Supporting Information

The Supporting Information is available free of charge on the ACS Publications website at DOI: 10.1021/acsmedchemlett.7b00456.

General information on materials, experimental details for the printing, UV screening, cellular assays, and synthesis (PDF) (PDF)

■ AUTHOR INFORMATION

Corresponding Authors

*E-mail: vincenzo.taresco@nottingham.ac.uk.
*E-mail: cameron.alexander@nottingham.ac.uk.

ORCID

Martin C. Garnett: 0000-0002-4365-4499
Vincenzo Taresco: 0000-0003-4476-8233
Cameron Alexander: 0000-0001-8337-1875

Notes

The authors declare no competing financial interest.
All raw data created during this research are openly available from the corresponding authors and at the University of Nottingham Research Data Management Repository (https://rdmc.nottingham.ac.uk).

■ ACKNOWLEDGMENTS

We thank EPSRC (Grants EP/N03371X/1, EP/H005625/1, EP/N006615/1, and EP/L013835/1) and the Royal Society (Wolfson Research Merit Award WM150086) for funding this work. We gratefully acknowledge Paul Cooling, Esme Ireson, Tom Booth, and Christine Grainger-Boultby for expert technical assistance. We thank Valentina Cuzzucoli Crucitti for graphical and picture design.

■ ABBREVIATIONS

p[3,4]p, pyrazolo[3,4-*d*]pyrimidines; PVPVA, polyvinylpyrrolidone-vinyl acetate copolymer; PVP, polyvinylpyrrolidone; HPMC, hydroxypropyl-methyl cellulose; PEG8000, polyethylene glycol 8000; PEG20000, polyethylene glycol 20000; Tween 80, surfactant; Pluronic F-68, surfactant; DMSO, dimethyl sulfoxide; *A*0, UV−vis absorbance; DLS, dynamic light scattering; MTT, methylthiazolyldiphenyl-tetrazolium bromide

■ REFERENCES

(1) Schenone, S.; Radi, M.; Musumeci, F.; Brullo, C.; Botta, M. Biologically driven synthesis of pyrazolo[3,4-*d*]pyrimidines as protein kinase inhibitors: an old scaffold as a new tool for medicinal chemistry and chemical biology studies. *Chem. Rev.* **2014**, *114*, 7189−7238.
(2) Ghozlan, S. A. S.; Abdelrazek, F. M.; Mohamed, M. H.; Azmy, K. E. Synthesis of some new pyrazole and pyrazolopyrimidine derivatives. *J. Heterocycl. Chem.* **2010**, *47*, 1379−1385.
(3) Todorovic, N.; Awuah, E.; Shakya, T.; Wright, G. D.; Capretta, A. Microwave-assisted synthesis of N1- and C3-substituted pyrazolo[3,4-*d*]pyrimidine libraries. *Tetrahedron Lett.* **2011**, *52*, 5761−5763.
(4) Liu, J.; Wang, X. Microwave-assisted, divergent solution-phase synthesis of 1,3,6-trisubstituted pyrazolo[3,4-*d*]pyrimidines. *ACS Comb. Sci.* **2011**, *13*, 414−420.
(5) Slavish, P. J.; Price, J. E.; Hanumesh, P.; Webb, T. R. Efficient synthesis of pyrazolopyrimidine libraries. *J. Comb. Chem.* **2010**, *12*, 807−809.
(6) Radi, M.; Dreassi, E.; Brullo, C.; Crespan, E.; Tintori, C.; Bernardo, V.; Valoti, M.; Zamperini, C.; Daigl, H.; Musumeci, F.; Carraro, F.; Naldini, A.; Filippi, I.; Maga, G.; Schenone, S.; Botta, M. Design, synthesis, biological activity, and ADME properties of pyrazolo[3,4-*d*]pyrimidines active in hypoxic human leukemia cells: a lead optimization study. *J. Med. Chem.* **2011**, *54*, 2610−2626.
(7) Tintori, C.; La Sala, G.; Vignaroli, G.; Botta, L.; Fallacara, A. L.; Falchi, F.; Radi, M.; Zamperini, C.; Dreassi, E.; Dello Iacono, L.; Orioli, D.; Biamonti, G.; Garbelli, M.; Lossani, A.; Gasparrini, F.; Tuccinardi, T.; Laurenzana, I.; Angelucci, A.; Maga, G.; Schenone, S.; Brullo, C.; Musumeci, F.; Desogus, A.; Crespan, E.; Botta, M. Studies on the ATP binding site of Fyn kinase for the identification of new

DOI: 10.1021/acsmedchemlett.7b00456
ACS Med. Chem. Lett. 2018, 9, 193−197

inhibitors and their evaluation as potential agents against tauopathies and tumors. *J. Med. Chem.* **2015**, *58*, 4590−4609.
(8) Ortuso, F.; Amato, R.; Artese, A.; D'antona, L.; Costa, G.; Talarico, C.; Gigliotti, F.; Bianco, C.; Trapasso, F.; Schenone, S.; Musumeci, F.; Botta, L.; Perrotti, N.; Alcaro, S. In silico identification and biological evaluation of novel selective serum/glucocorticoid-inducible kinase 1 inhibitors based on the pyrazolo-pyrimidine scaffold. *J. Chem. Inf. Model.* **2014**, *54*, 1828−1832.
(9) Radi, M.; Brullo, C.; Crespan, E.; Tintori, C.; Musumeci, F.; Biava, M.; Schenone, S.; Dreassi, E.; Zamperini, C.; Maga, G.; Pagano, D.; Angelucci, A.; Bologna, M.; Botta, M. Identification of potent c-Src inhibitors strongly affecting the proliferation of human neuroblastoma cells. *Bioorg. Med. Chem. Lett.* **2011**, *21*, 5928−5933.
(10) Radi, M.; Tintori, C.; Musumeci, F.; Brullo, C.; Zamperini, C.; Dreassi, E.; Fallacara, A. L.; Vignaroli, G.; Crespan, E.; Zanoli, S.; Laurenzana, I.; Filippi, I.; Maga, G.; Schenone, S.; Angelucci, A.; Botta, M. Design, synthesis, and biological evaluation of pyrazolo[3,4-*d*]pyrimidines active in vivo on the Bcr-Abl T315I mutant. *J. Med. Chem.* **2013**, *56*, 5382−5394.
(11) Ceccherini, E.; Indovina, P.; Zamperini, C.; Dreassi, E.; Casini, N.; Cutaia, O.; Forte, I. M.; Pentimalli, F.; Esposito, L.; Polito, M. S.; Schenone, S.; Botta, M.; Giordano, A. SRC family kinase inhibition through a new pyrazolo[3,4-*d*]pyrimidine derivative as a feasible approach for glioblastoma treatment. *J. Cell. Biochem.* **2015**, *116*, 856−863.
(12) Casini, N.; Forte, I. M.; Mastrogiovanni, G.; Pentimalli, F.; Angelucci, A.; Festuccia, C.; Tomei, V.; Ceccherini, E.; Di Marzo, D.; Schenone, S.; Botta, M.; Giordano, A.; Indovina, P. SRC family kinase (SFK) inhibition reduces rhabdomyosarcoma cell growth in vitro and in vivo and triggers p38 MAP kinase-mediated differentiation. *Oncotarget* **2015**, *6*, 12421−12435.
(13) Spreafico, A.; Schenone, S.; Serchi, T.; Orlandini, M.; Angelucci, A.; Magrini, D.; Bernardini, G.; Collodel, G.; Di Stefano, A.; Tintori, C.; Bologna, M.; Manetti, F.; Botta, M.; Santucci, A. Antiproliferative and proapoptotic activities of new pyrazolo[3,4-*d*]pyrimidine derivative Src kinase inhibitors in human osteosarcoma cells. *FASEB J.* **2008**, *22*, 1560−1571.
(14) Angelucci, A.; Schenone, S.; Gravina, G. L.; Muzi, P.; Festuccia, C.; Vicentini, C.; Botta, M.; Bologna, M. Pyrazolo[3,4-*d*]pyrimidines c-Src inhibitors reduce epidermal growth factor-induced migration in prostate cancer cells. *Eur. J. Cancer* **2006**, *42*, 2838−2845.
(15) Indovina, P.; Giorgi, F.; Rizzo, V.; Khadang, B.; Schenone, S.; Di Marzo, D.; Forte, I. M.; Tomei, V.; Mattioli, E.; D'Urso, V.; Grilli, B.; Botta, M.; Giordano, A.; Pentimalli, F. New pyrazolo[3,4-*d*]pyrimidine Src inhibitors induce apoptosis in mesothelioma cell lines through p27 nuclear stabilization. *Oncogene* **2012**, *31*, 929−938.
(16) Dreassi, E.; Zizzari, A. T.; Mori, M.; Filippi, I.; Belfiore, A.; Naldini, A.; Carraro, F.; Santucci, A.; Schenone, S.; Botta, M. 2-Hydroxypropyl-*β*-cyclodextrin strongly improves water solubility and anti-proliferative activity of pyrazolo[3,4-*d*]pyrimidines Src-Abl dual inhibitors. *Eur. J. Med. Chem.* **2010**, *45*, 5958−5964.
(17) Vignaroli, G.; Calandro, P.; Zamperini, C.; Coniglio, F.; Iovenitti, G.; Tavanti, M.; Colecchia, D.; Dreassi, E.; Valoti, M.; Schenone, S.; Chiariello, M.; Botta, M. Improvement of pyrazolo[3,4-*d*]pyrimidines pharmacokinetic properties: nanosystem approaches for drug delivery. *Sci. Rep.* **2016**, *6*, 21509.
(18) Fallacara, A. L.; Mancini, A.; Zamperini, C.; Dreassi, E.; Marianelli, S.; Chiariello, M.; Pozzi, G.; Santoro, F.; Botta, M.; Schenone, S. Pyrazolo[3,4-*d*]pyrimidines-loaded human serum albumin (HSA) nanoparticles: preparation, characterization and cytotoxicity evaluation against neuroblastoma cell line. *Bioorg. Med. Chem. Lett.* **2017**, *27*, 3196−3200.
(19) Vignaroli, G.; Zamperini, C.; Dreassi, E.; Radi, M.; Angelucci, A.; Sanità, P.; Crespan, E.; Kissova, M.; Maga, G.; Schenone, S.; Musumeci, F.; Botta, M. Pyrazolo[3,4-*d*]pyrimidine prodrugs: strategic optimization of the aqueous solubility of dual Src/Abl inhibitors. *ACS Med. Chem. Lett.* **2013**, *4*, 622−626.
(20) Baghel, S.; Cathcart, H.; O'Reilly, N. J. Polymeric amorphous solid dispersions: a review of amorphization, crystallization, stabilization, solid-state characterization, and aqueous solubilization of biopharmaceutical classification system class II drugs. *J. Pharm. Sci.* **2016**, *105*, 2527−2544.
(21) Vo, C. L.-N.; Park, C.; Lee, B.-J. Current trends and future perspectives of solid dispersions containing poorly water-soluble drugs. *Eur. J. Pharm. Biopharm.* **2013**, *85*, 799−813.
(22) Huang, Y.; Dai, W.-G. Fundamental aspects of solid dispersion technology for poorly soluble drugs. *Acta Pharm. Sin. B* **2014**, *4*, 18−25.
(23) Van Eerdenbrugh, B.; Taylor, L. S. Small scale screening to determine the ability of different polymers to inhibit drug crystallization upon rapid solvent evaporation. *Mol. Pharmaceutics* **2010**, *7*, 1328−1337.
(24) Taresco, V.; Louzao, I.; Scurr, D.; Booth, J.; Treacher, K.; McCabe, J.; Turpin, E.; Laughton, C. A.; Alexander, C.; Burley, J. C.; Garnett, M. C. Rapid nanogram scale screening method of microarrays to evaluate drug-polymer blends using high-throughput printing technology. *Mol. Pharmaceutics* **2017**, *14*, 2079−2087.
(25) Chelli, B.; Maga, G.; Bondavalli, F.; Botta, M.; Crespan, E.; Mosci, F.; Martini, C.; Brullo, C.; Manetti, F.; Bruno, O.; Magnani, M. B.; Trincavelli, M. L.; Carraro, F.; Schenone, S.; Naldini, A. Structure-based optimization of pyrazolo[3,4-*d*]pyrimidines as Abl inhibitors and antiproliferative agents toward human leukemia cell lines. *J. Med. Chem.* **2008**, *51*, 1252−1259.
(26) Kruewel, T.; Schenone, S.; Radi, M.; Maga, G.; Rohrbeck, A.; Botta, M.; Borlak, J. Molecular characterization of c-Abl/c-Src kinase inhibitors targeted against murine tumour progenitor cells that express stem cell markers. *PLoS One* **2010**, *5*, e14143.
(27) Sivina, M.; Kreitman, R. J.; Arons, E.; Ravandi, F.; Burger, J. A. The BTK inhibitor Ibrutinib (PCI-32765) blocks hairy cell leukaemia survival, proliferation and Bcr signalling: a new therapeutic approach. *Br. J. Haematol.* **2014**, *166*, 177−188.

DOI: 10.1021/acsmedchemlett.7b00456
ACS Med. Chem. Lett. 2018, 9, 193−197